

Supporting information

Two-dimensional metal-organic frameworks nanosheets for highly efficient electrocatalytic biomass 5-(hydroxymethyl)furfural (HMF) valorization

Mengke Cai,^{+,a} Yawei Zhang,^{+,a} Yiyue Zhao,^a Qinglin Liu,^a Yinle Li,^a and Guangqin Li^{*,a}

^a MOE Laboratory of Bioinorganic and Synthetic Chemistry, Lehn Institute of Functional Materials, School of Chemistry, Sun Yat-Sen University, Guangzhou 510275, P. R. China.

* Corresponding author. E-mail address: liguangqin@mail.sysu.edu.cn (G. Li)

⁺ M. C and Y. Z contributed equally to this work.

Number of pages: 16

Number of tables: 4

Number of figures: 13

Table of contents

Section 1	Experimental Section	S3-S4
Section 2	HPLC Standard Plots and HMF Stable Tests	S5-S6
Section 3	XRD, Crystal Structure Diagram and Elemental Ratios	S6-8
Section 4	Electrochemical Tests for HMF Oxidation	S9-S12
Section 5	Comparison of Electrochemical Performance	S13-S14
Section 6	Electrocatalytic Stability	S15-S16
Reference		S16

Section 1: *Experimental Section*

Chemical and Materials. Sodium hydroxide (NaOH, AR95%), terephthalic acid (BDC, AR98%), nickel nitrate hexahydrate ($\text{Ni}(\text{NO}_3)_2 \cdot 6\text{H}_2\text{O}$, AR98%), cobalt nitrate hexahydrate ($\text{Co}(\text{NO}_3)_2 \cdot 6\text{H}_2\text{O}$, AR98%), manganese nitrate tetrahydrate ($\text{Mn}(\text{NO}_3)_2 \cdot 4\text{H}_2\text{O}$, AR98%), iron nitrate nonahydrate ($\text{Fe}(\text{NO}_3)_3 \cdot 9\text{H}_2\text{O}$, AR98%), *N, N*-dimethylformamide (DMF, AR99%), 5-(hydroxymethyl)furfural (HMF), 2,5-furandicarboxylic acid (FDCA, AR95%), 5-formyl-2-furancarboxylic acid (FFCA, AR95%), 5-hydroxymethyl-2-furancarboxylic acid (HMFCa, AR95%), ammonium formate (HCOONH_4 , AR99%) and ethanol (EtOH, AR99%) were purchased from Sigma-Aldrich and were used as purchased without further purification. Deionized water (resistivity > 18 M Ω cm) was used in all experiments from a Sartorius Arium comfort I system. Nickel foams (NF) was ultrasonically washed with HCl solution (2 M) for 15 min.

Synthesis of NiBDC-NF. Terephthalic acid (166 mg, 1.0 mmol) and nickel nitrate hexahydrate (146 mg, 0.5 mmol) were dissolved in 10 mL *N, N*-dimethylformamide (DMF) and 2 mL deionized water under stirring in a 15 mL glass bottle with closed lid. Then a piece of NF (1 cm \times 4 cm) was placed in it. After that, the glass bottle was heated with oil bath for 15 h at 100 °C. The resulting NiBDC-NF was washed with DMF and ethanol three times and dried naturally.

Synthesis of NiMBDC-NF (M = Co, Fe, Mn). The synthesis of NiMBDC-NF was similar to that of NiBDC-NF, but using $\text{Ni}(\text{NO}_3)_2 \cdot 6\text{H}_2\text{O}$ (131 mg, 0.45 mmol) and $\text{Co}(\text{NO}_3)_2 \cdot 6\text{H}_2\text{O}$ (15 mg, 0.05 mmol) to replace $\text{Ni}(\text{NO}_3)_2 \cdot 6\text{H}_2\text{O}$ (146 mg, 0.5 mmol) for the synthesis of NiCoBDC-NF, using $\text{Ni}(\text{NO}_3)_2 \cdot 6\text{H}_2\text{O}$ (131 mg, 0.45 mmol) and $\text{Fe}(\text{NO}_3)_3 \cdot 9\text{H}_2\text{O}$ (20 mg, 0.05 mmol) for the synthesis of NiFeBDC-NF, using $\text{Ni}(\text{NO}_3)_2 \cdot 6\text{H}_2\text{O}$ (130 mg, 0.45 mmol) and $\text{Mn}(\text{NO}_3)_2 \cdot 4\text{H}_2\text{O}$ (12.5 mg, 0.05 mmol) for the synthesis of NiMnBDC-NF.

Materials Characterizations. Scan field-emission scanning electron microscopy (FESEM) images were performed on a Hitachi SU8010 scanning electron microscope at 5.0 kV. Transmission electron microscopy (TEM) images were carried out using JEOL JEM-1400 at 120 kV. High angle annular dark field scanning transmission electron microscopy (HAADF-SEM) imaging and energy-dispersive X-ray spectroscopy (EDXS) elemental mapping were carried out on JEOL ARM200 at 300 kV. X-ray diffraction (XRD) patterns were recorded on a Rigaku SmartLab diffractometer with $\text{Cu K}\alpha$ ($\lambda = 1.540598 \text{ \AA}$) radiation operating at 30 kV and 200 mA. X-ray photoelectron spectroscopy (XPS) was performed by a VG ESCALABMKII instrument. The N_2 adsorption-desorption isotherms were collected using a Quantachrome Instruments Autosorb-iQ2-MP at 77 K. The high performance liquid chromatography (HPLC) was conducted by Waters 1525.

Electrochemical Measurements. A three-electrode glass cell with a electrolyte of pH13, a platinum wire counter electrode, an Ag/AgCl reference electrode and glassy carbon (GC) working electrode on CHI 760E electrochemistry workstation. The measured potentials versus the reversible hydrogen electrode (RHE) were converted according to the equation

(1): $E_{\text{RHE}} = E_{\text{Ag/AgCl}} + 0.197 + 0.059 \times \text{pH}$ (1). The 2D MOFs loaded on NF were directly used as a working electrode immersed in electrolyte (20 mL) with 1 cm × 1 cm area. LSV curves were recorded at a scan rate of 5 mV/s. The potential in the LSV polarization curves were corrected without iR compensate. The electrochemical active surface areas (ECSA) were evaluated by measuring the double-layer capacitance (Cdl) via cyclic voltammograms (CV) at different scan rates. The CV was measured in the potential range from 1.36 to 1.46 V vs RHE at different scan rate.

HPLC analysis. 20 µL aliquot was periodically collected from the electrolyte solution during chronoamperometry and then was diluted with 980 µL of water. After that, supernatant after centrifugation was then analyzed via HPLC at room temperature to calculate the reactant HMF and products content. The HPLC instrument was equipped with an ultraviolet-visible detector set at 265 nm and a 4.6 mm × 150 mm Shim-pack GWS 5 µm C18 column. The eluent solvent is a mixture of 5 mM ammonium formate aqueous solution and methanol. Separation was accomplished using an equal elution by fixing the volume percentage of methanol 30 % during 0 to 5 min and the flow rate was set at 0.5 mL/min. A volume of three times the volume of the injection loop (10 µL) was injected. The quantification of HMF electrooxidation was calculated based on the calibration curves of those standard compounds purchased from commercial vendors. FDCA yield, FDCA yield rate, FDCA selectivity and faradaic efficiency were calculated according to equations (2), (3), (4) and (5), respectively.

$$\text{FDCA yield} = n(\text{FDCA formed}) / n(\text{HMF initial}) \quad (2)$$

$$\text{FDCA yield rate} = n(\text{FDCA formed}) / [s(\text{electrode area}) / t(\text{electrolysis time})] \quad (3)$$

$$\text{FDCA selectivity (\%)} = [n(\text{FDCA formed}) / n(\text{HMF consumed})] \times 100 \quad (4)$$

$$\text{faradaic efficiency (\%)} = [n(\text{FDCA formed}) / (\text{Charge} / (6 \times F))] \times 100 \quad (5)$$

with F being the Faraday constant (96485 C mol⁻¹) and n as the mol of reactant calculated from the concentration measured by HPLC.

HPLC analysis of HMF degradation. The degradation of HMF in alkaline solution was measured in KOH solution with pH 14, pH 13.5 and pH 13, in the presence of 10 and 5 mM HMF at 25 °C. Samples were taken directly after the addition of HMF, and after 1, 2, 4, and 6 hours. The samples were injected into the HPLC system after dilution with 990 µL water.

Section 2: HPLC Standard Plots and HMF Stable Tests

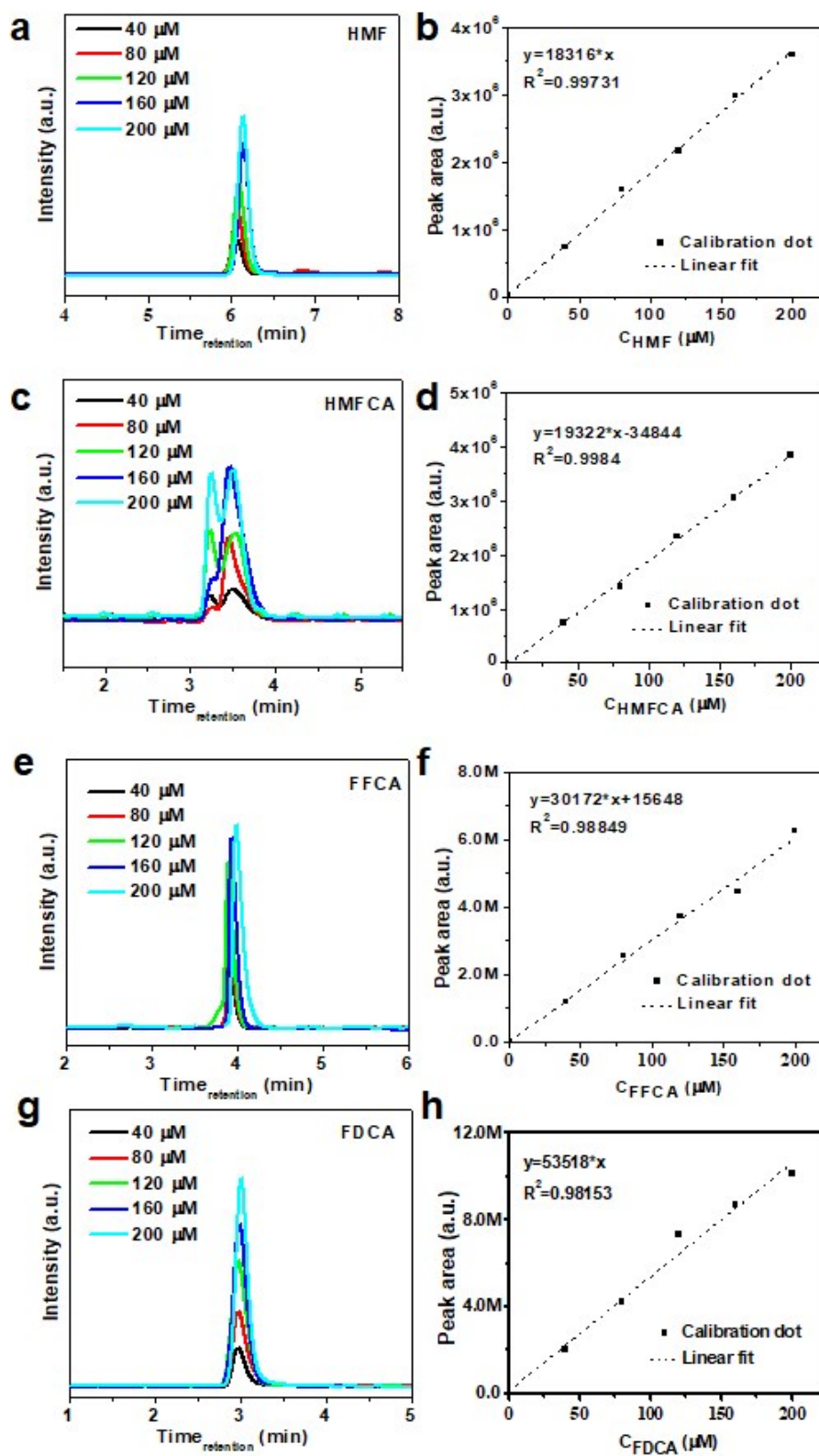


Figure S1. HPLC measurements and linear plots of pure HMF, FDCA and intermediates.

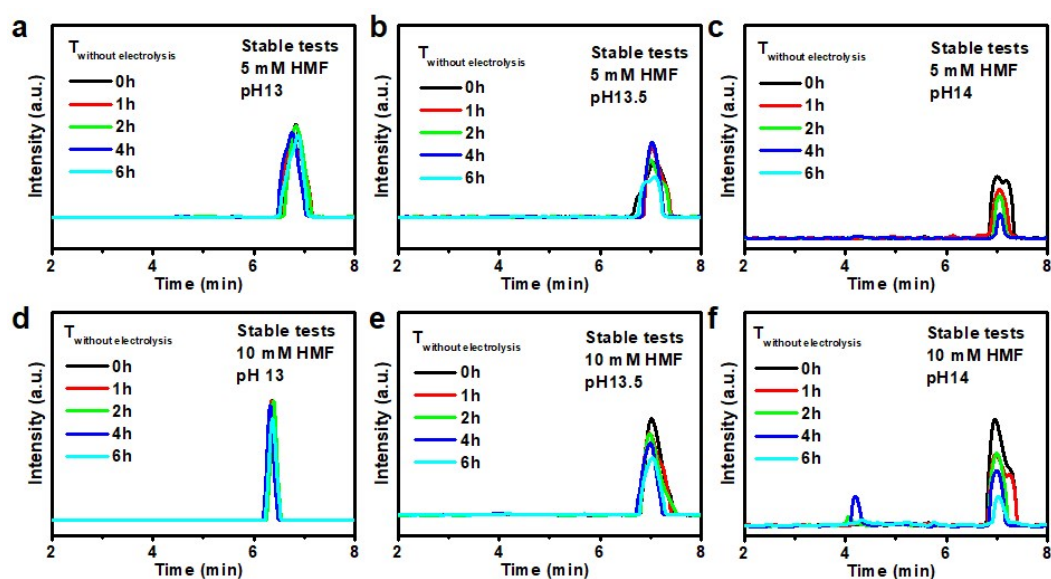


Figure S2. HMF stable tests. HPLC chromatograms at various test times with different HMF concentrations and pH.

Section 3: XRD, Crystal Structure Diagram and Elemental Ratios

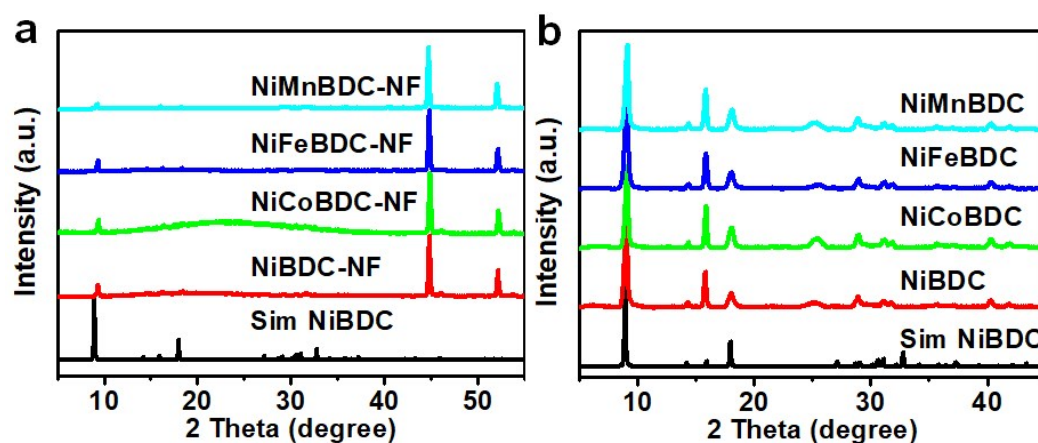


Figure S3. XRD patterns of the prepared (a) NiBDC-NF and doped NiMBDC-NF, (b) the corresponding pure powder after removed from nickel foam.

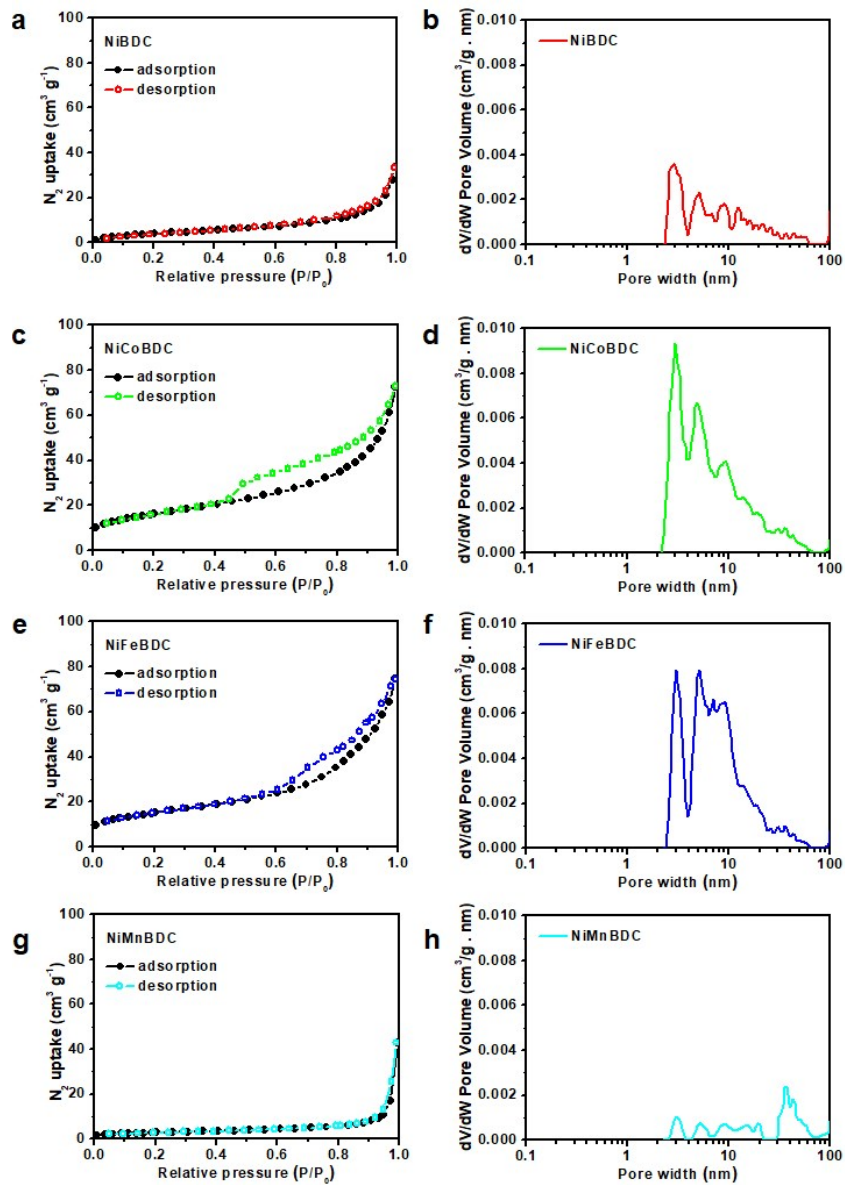


Figure S4. Nitrogen (77K) adsorption-desorption isotherms and pore size distribution based on nonlocal density functional theory (NLDFT) of (a, b) NiBDC, (c, d) NiCoBDC, (e, f) NiFeBDC and (g, h) NiMnBDC.

Table S1. Comparison of specific surface area and total pore volume for prepared samples.

NiBDC samples	Specific surface area ($\text{m}^2 \text{g}^{-1}$)	Total pore volume ($\text{cm}^3 \text{g}^{-1}$)
NiBDC	13.2	0.034
NiCoBDC	47.7	0.065
NiFeBDC	35.4	0.082

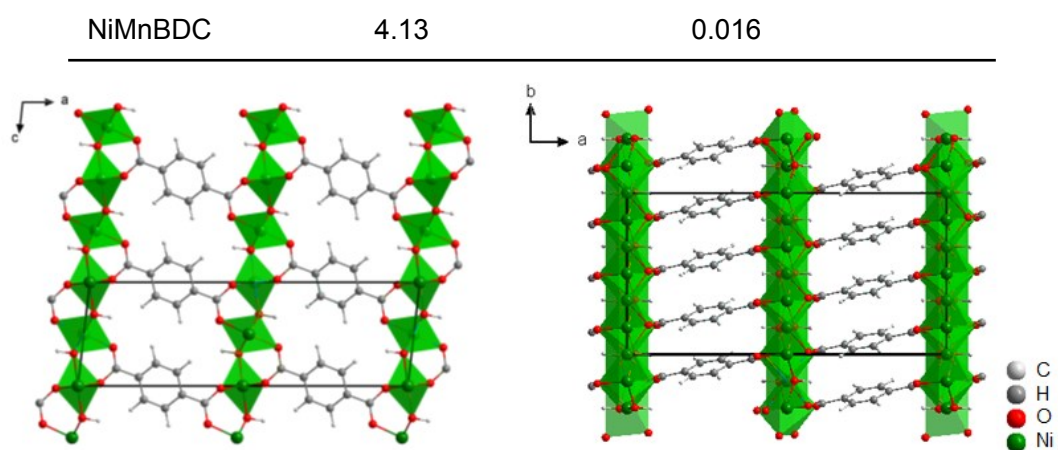


Figure S5. Crystal structure diagram of the 2D MOFs NiBDC with the molecular formula of $[\text{Ni}_3(\text{OH})_2(1,4\text{-BDC})_2(\text{H}_2\text{O})_4] \cdot 2\text{H}_2\text{O}$.

Table S2. Elemental ratios and Ni/M-doped ratios of prepared samples.

Samples	C Atom %	O Atom %	Ni Atom %	M-doped Atom %	Ni/M-doped
NiBDC	79.5	18.5	2.0	\	\
NiCoBDC	78.3	19.5	2.0	0.2	10:1
NiFeBDC	78.5	19.4	1.9	0.2	9.5:1
NiMnBDC	86.4	12.5	1.0	0.1	10:1

Section 4: Electrochemical Tests for HMF Oxidation

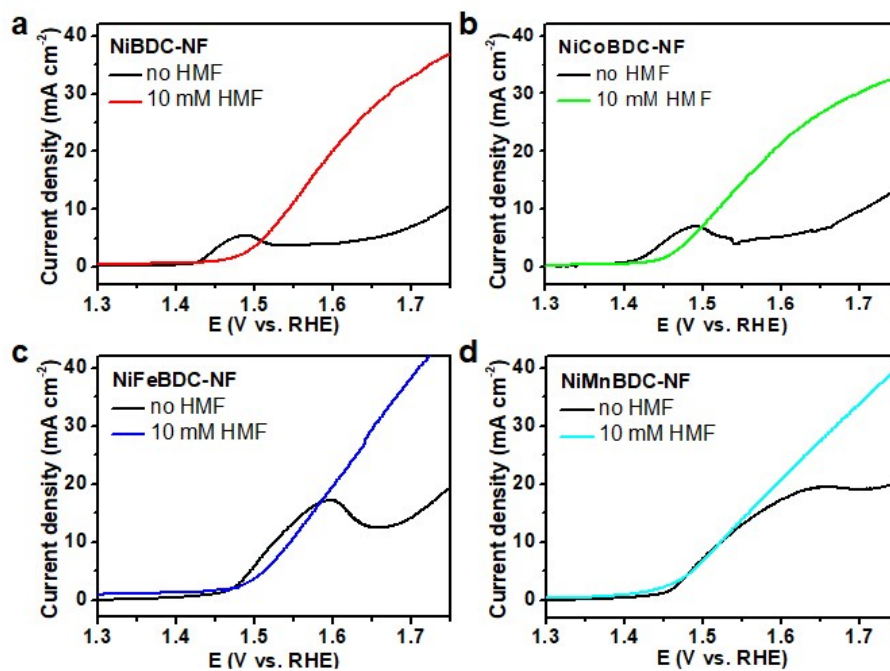


Figure S6. The LSV for the NiBDC-NF and the other metal-doped samples at a scan rate of 5 mV s^{-1} in 0.1 M KOH without and with 10 mM HMF .

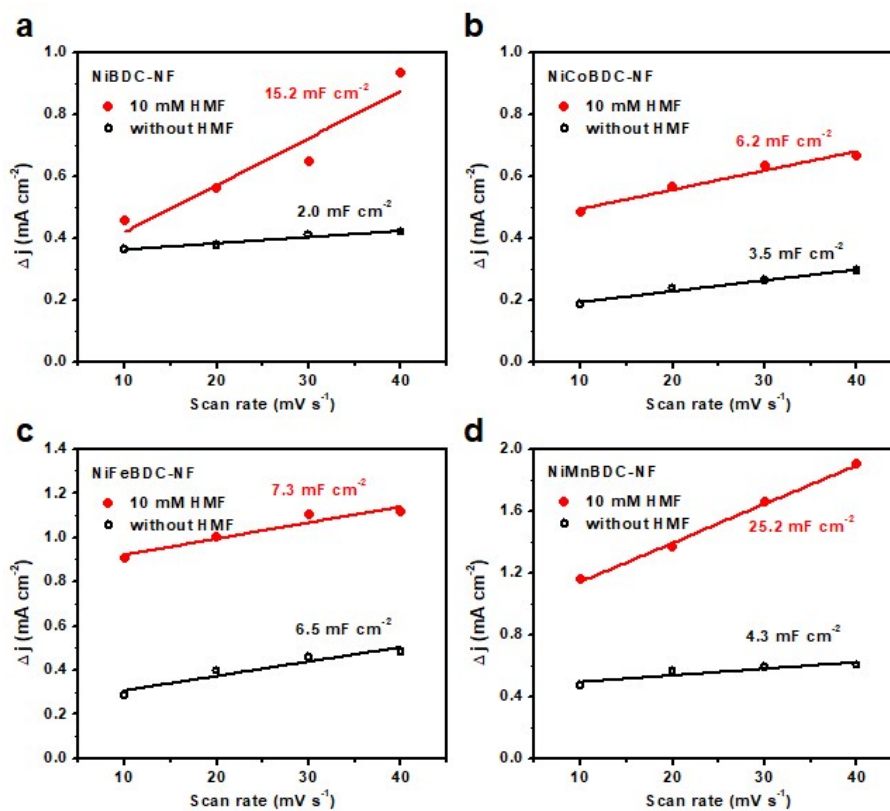


Figure S7. The current density plotted against scan rates without and with 10 mM HMF for the NiBDC-NF and the other metal-doped samples at 1.42 V (vs RHE).

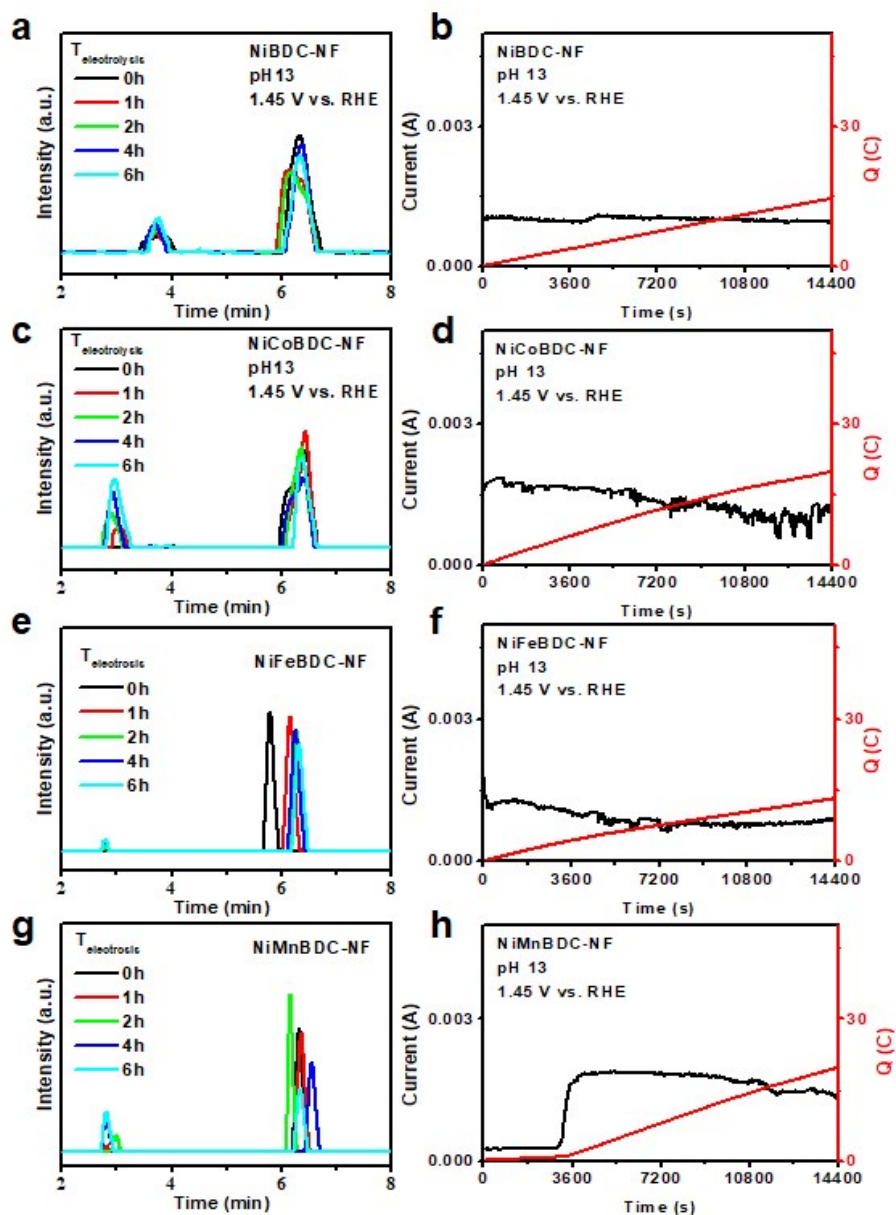


Figure S8. FDCA electrooxidation test applied on 1.45 V vs RHE. (a, c, e, g) The HPLC chromatograms at various electrolysis times. (b, d, f, h) Corresponding current-time and charge-time plots during constant potential electrolysis of a 20 mL solution of 10 mM HMF in 0.1 M KOH using four as-prepared catalysts.

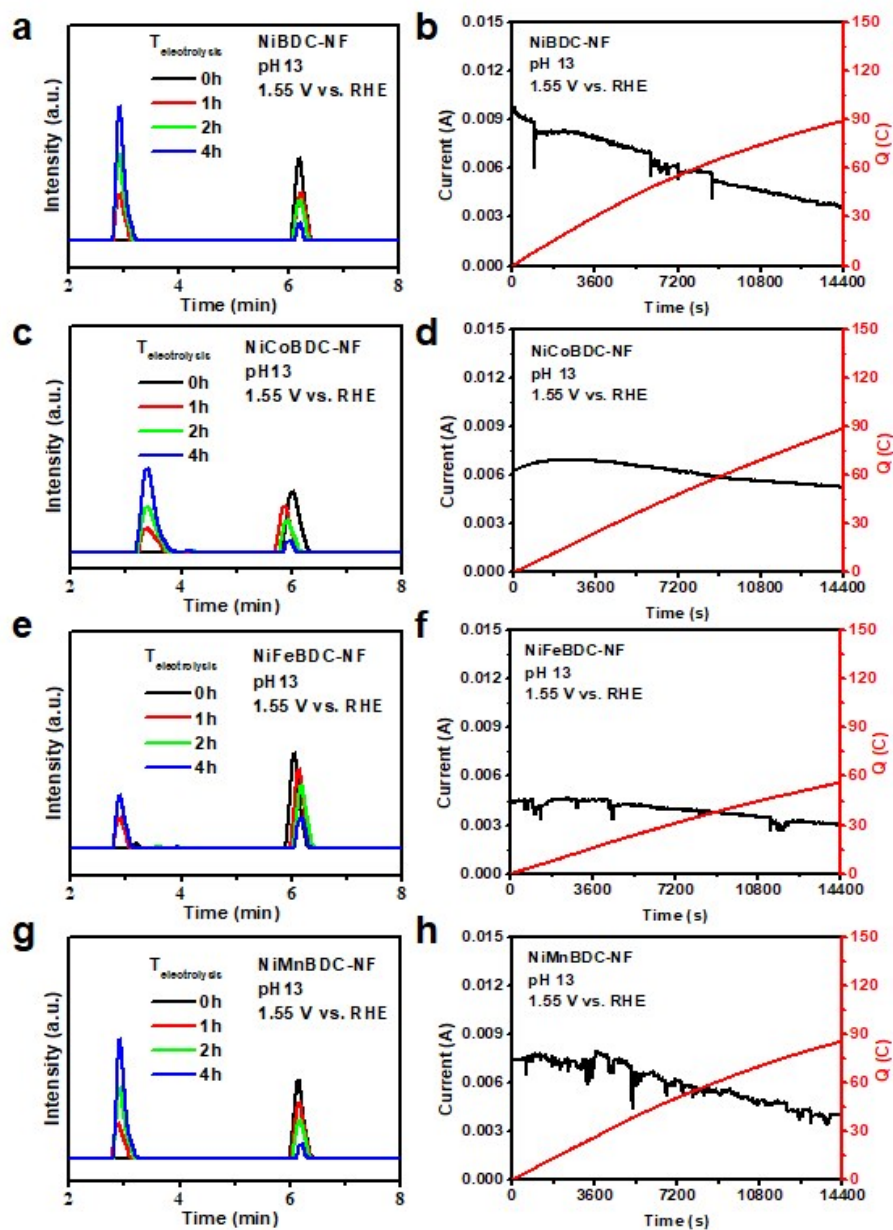


Figure S9. FDCA electrooxidation test applied on 1.55 V vs RHE. (a, c, e, g) The HPLC chromatograms at various electrolysis times. (b, d, f, h) Corresponding current-time and charge-time plots during constant potential electrolysis of a 20 mL solution of 10 mM HMF in 0.1 M KOH using four as-prepared catalysts.

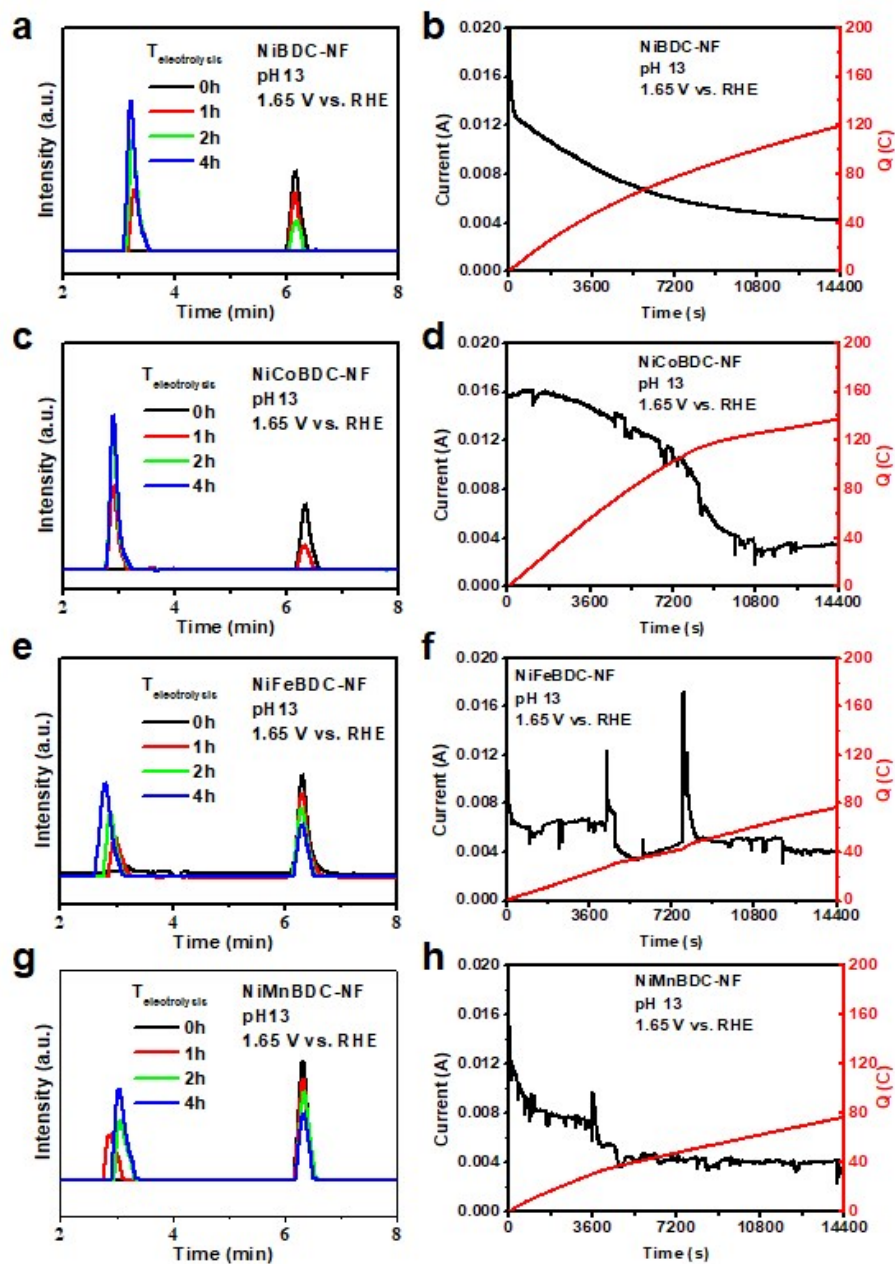


Figure S10. FDCA electrooxidation test applied on 1.65 V vs RHE. (a, c, e, g) The HPLC chromatograms at various electrolysis times. (b, d, f, h) Corresponding current-time and charge-time plots during constant potential electrolysis of a 20 mL solution of 10 mM HMF in 0.1 M KOH using four as-prepared catalysts.

Section 5: Comparison of Electrochemical Performance

Table S3. HMF electrooxidation performance of prepared samples.

BDC-NF	pH	E vs RHE	T/h	FDCA(yield) $\mu\text{mol cm}^{-2} \text{h}^{-1}$	Faraday efficiency	FDCA(yield) %
Ni	13	1.45	1	4.47	86.4%	5.5
Ni	13	1.55	1	16.7	62.3%	20.8
Ni	13	1.65	1	28.7	53.5%	35.8
NiCo	13	1.45	1	7.08	99.9%	8.8
NiCo	13	1.55	1	23.3	83.1%	29.1
NiCo	13	1.65	1	40.0	62.0%	50.0
NiFe	13	1.45	1	2.92	86.6%	3.6
NiFe	13	1.55	1	9.79	53.1%	12.2
NiFe	13	1.65	1	16.0	60.7%	20.0
NiMn	13	1.45	1	1.24	83.0%	1.5
NiMn	13	1.55	1	16.6	54.9%	20.7
NiMn	13	1.65	1	14.9	42.6%	18.6
Ni	13	1.45	4	3.05	73.6%	15.2
Ni	13	1.55	4	11.9	36.0%	59.5
Ni	13	1.65	4	16.4	47.7%	82.0
NiCo	13	1.45	4	4.53	92.6%	22.6
NiCo	13	1.55	4	20.1	78.8%	99.0
NiCo	13	1.65	4	18.0	45.6%	90.0
NiFe	13	1.45	4	1.67	82.6%	8.3
NiFe	13	1.55	4	8.87	54.9%	44.3
NiFe	13	1.65	4	10.9	49.6%	54.5
NiMn	13	1.45	4	3.69	65.1%	18.4
NiMn	13	1.55	4	12.8	52.0%	64.0
NiMn	13	1.65	4	7.99	36.3%	39.9

Table S4. HMF electrooxidation performance of reported catalysts when pH < 14 is performed as electrocatalytic conditions.

Published year	Catalyst	V(HMF)	C(HMF)	pH	E vs RHE	Yield	FE	Cell	Ref.
-	NiCoBDC-NF	20mL	10mM	13	1.55	29% 99%	83.1/1h 78.8/4h	H-cell	this work
2012	Pt/C	50mL	-	10	-	80%	-	H-cell	1
2014	PdAu/C	50mL	20mM	13	0.9	83%	-	Flow-cell	2
2015	Au(TEMPO)	-	5mM	9.2	1.54	≥99%	≥93	H-cell	3
2018	MnO _x	15mL	20mM	1	1.6	53.8%	33.8	H-cell	4
2018	Nanocrystalline Cu Foam	14mL	5mM	13	1.62	96.4%	>95	H-cell	5
2018	NiCo ₂ O ₄	-	10mM	13	1.55	90%	92–99	H-cell	6
2019	Ag/C	-	-	12	1.55	98%	≈ 80	H-cell	7
2019	NiOOH	14mL	5mM	13	1.47	96.0%	96	H-cell	8
	CoOOH				1.56	35.1%	35.1		
	FeOOH				1.71	1.6%	1.59		
2019	Glassy carbon(ACT\TEMPO)	-	20mM	10	1.4	93.5%	93.5	H-cell	9

Section 6: Electrocatalytic Stability

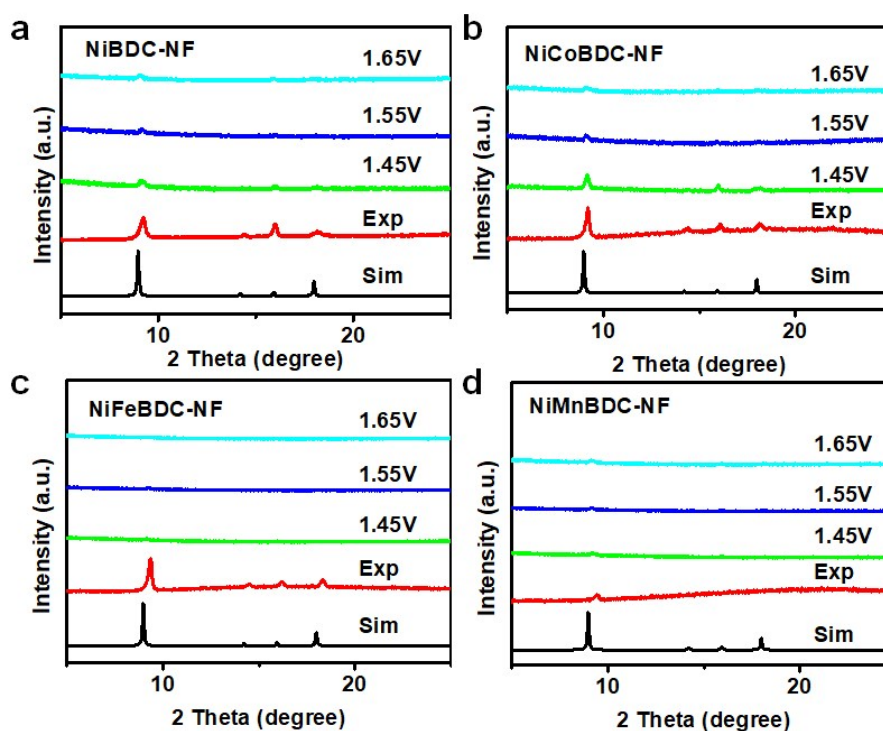


Figure S11. Comparison of XRD patterns before and after 4 h electrolysis for four as-prepared catalysts.

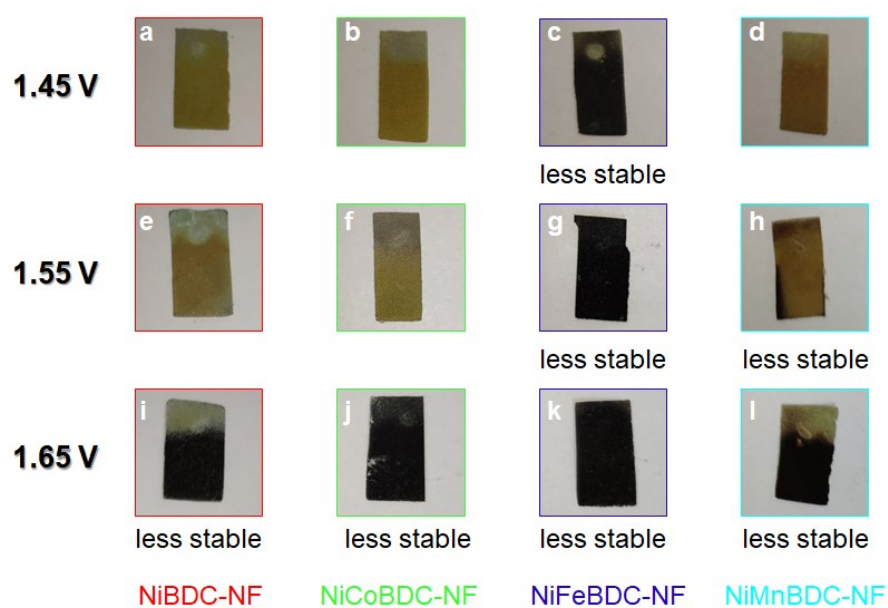


Figure S12. Comparison of sample images after 4 h electrolysis for four as-prepared catalysts.

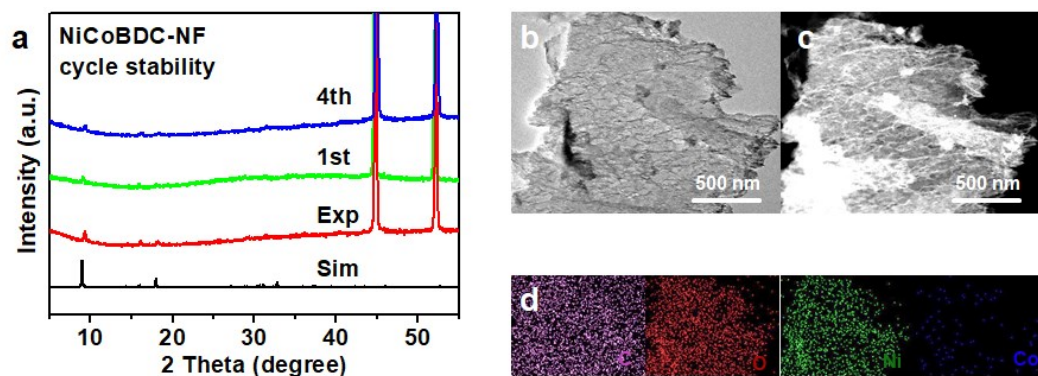


Figure S13. Stable tests of four successive electrolysis for NiCoBDC-NF. (a) Comparison of XRD patterns of the pristine and post sample after the 1st and 4th cycle tests. (b) TEM, (c) HAADF-STEM and (d) elemental mapping images after four cycle tests.

Reference

1. K. R. Vuyyuru and P. Strasser, *Catalysis Today*, 2012, 195, 144-154.
2. D. J. Chadderdon, L. Xin, J. Qi, Y. Qiu, P. Krishna, K. L. More and W. Li, *Green Chemistry*, 2014, 16, 3778-3786.
3. H. G. Cha and K. S. Choi, *Nature chemistry*, 2015, 7, 328-333.
4. S. R. Kubota and K. S. Choi, *ChemSusChem*, 2018, 11, 2138-2145.
5. D.-H. Nam, B. J. Taitt and K.-S. Choi, *ACS Catal.*, 2018, 8, 1197-1206.
6. L. Gao, Y. Bao, S. Gan, Z. Sun, Z. Song, D. Han, F. Li and L. Niu, *ChemSusChem*, 2018, 11, 2547-2553.
7. X. H. Chadderdon, D. J. Chadderdon, T. Pfennig, B. H. Shanks and W. Li, *Green Chemistry*, 2019, 21, 6210-6219.
8. B. J. Taitt, D.-H. Nam and K.-S. Choi, *ACS Catal.*, 2018, 9, 660-670.
9. A. C. Cardiel, B. J. Taitt and K.-S. Choi, *ACS Sustainable Chem. Eng.*, 2019, 7, 11138-11149.